Supporting Information

Understanding the role of Ce sites for boosting PEC-NIRR without externally applied potentials

Lijing Liu[a†], Yajie Bai[a†], Zhenzhen Huang[c], Guanhua Wang[d] , Jianguo Cui[e], Hongye Bai[a,*] and Weiqiang Fan[a,b*]

[a] *School of Chemistry and Chemical Engineering, Jiangsu University, Zhenjiang, 212013, PR China.*

[b] *Synergistic Innovation Center of Modern Agricultural Equipment, Jiangsu University, Zhenjiang, 212013, PR China.*

[c] *College of Chemistry, Jilin University, Changchun 130012, P. R. China.*

[d] *College of Veterinary Medicine, South China Agricultural University, Guangzhou 510642, Guangdong, PR China.*

[e] *Baotou Research Institute of Rare Earths, Baotou 014030, PR China.*

† *These authors contributed equally to this work.*

* Corresponding author: bhy198412@163.com, fwq4993329@ujs.edu.cn

1. Experimental section

1.1. Chemical reagents

All chemical reagents were purchased from Sinopharm Chemical Reagent Co., Ltd. and were of analytical grade without further purification. The FTO glass substrates were sonicated with acetone, ethanol, and deionized water, respectively.

1.2. Synthesis of p-$BiVO_4$

2.9106 g $Bi(NO_3)_3 \cdot 5H_2O$ and 2.2332 g EDTA-2Na were dissolved in 60 mL HNO_3 solution (2 mol L^{-1}), which was recorded as solution A. 0.7014 g NH_4NO_3 and 2.2333 g EDTA-2Na were dissolved in 120 mL NaOH (1 mol L^{-1}), which was recorded as solution B. The above two solutions and FTO were added to stainless-steel Teflon-lined autoclave, and kept at 160 °C for 12 h. Finally, the synthesized p-$BiVO_4$ was washed with deionized water and dried in a 60 ℃ oven for 2 h.

1.3. Synthesis of xCe-$BiVO_4$

The preparation method of xCe-$BiVO_4$ is the same as that of p-$BiVO_4$, except that $Ce(NO_3)_3 \cdot 6H_2O$ was added. The molar ratios of Ce^{3+} and Bi^{3+} are 0.7%, 1.5% and 2.3%.

1.4. Characterizations

The crystal structures were tested by X-ray diffraction (XRD). The morphology was investigated by the scanning electron microscopy (FESEM), transmission electron microscopy (TEM), high-resolution TEM (HRTEM) and energy dispersive spectroscopy (EDS, XMAX50). The chemical valence was measured by X-ray photoelectron spectroscopy (XPS, ESCALABA 250XI). The UV-vis diffuse reflectance spectroscopy (DRS) was studied by UV–Vis diffuse reflectance spectroscopy. ^{1}H nuclear magnetic resonance (^{1}H NMR) of $^{14}NH_4^+$ and $^{15}NH_4^+$ was

detected by Bruker AVANCEIII 400 MHz spectrum. Raman spectra were measured on a DXR (Thermo Scientific) spectrometer.

1.5. PEC-NIRR experiment

The PEC-NIRR experiments were carried out in a three-electrode system, in which the sample was used as the working electrode, and the Pt sheet (1cm × 1cm) and Ag/AgCl (saturated KCl electrolyte) were used as the counter electrode and the reference electrode, respectively. 0.015 g $NaNO_3$ (150 μg mL^{-1}) was added to 0.5 M Na_2SO_4 solution (50 mL) as reactant, and the working electrode was irradiated under the 300 W xenon lamp (100 mW cm^{-2}). Linear-sweep-voltammetry (LSV) curves were scanned at a speed of 50 mV s^{-1}. The Mott-Schottky plots and photoelectrochemical impedance spectroscopy (EIS) data were measured in 0.5 M Na_2SO_4 solution. In addition, before the experiment, it is necessary to open the agitator, stir the reaction liquid at a certain speed, and continuously inject Ar gas into the electrolytic cell for 1 h to remove the dissolved N_2.

1.6. Analytical methods

Detection of NH_3: The yield of NH_3 was analyzed by Nessler's reagent. 5 mL reacted electrolyte, 0.1 mL potassium sodium tartrate ($KNaC_4H_6O_6 \cdot H_2O$, 0.5 g/mL) solution and 0.1 mL Nessler reagent were mixed together, and then the mixed solution stood for 10 min. The absorbance of the mixed solution was detected at 425 nm. Meanwhile, the standard curve was linearly fitted by different concentrations of NH_4Cl solution, and the corresponding absorbance (y = 0.12888x + 0.01022) is shown in Fig. S13.

Detection of NO_3^-:

5 mL reacted electrolyte, 0.1 mL HCl (1 M) and 0.3 mL sulfamic acid solution (0.8 wt%) were mixed together, and then the mixed solution stood for 10 min. The absorbance of the mixed solution was detected in the range of 225 nm – 275 nm. The

standard curve was obtained by linear fitting of $NaNO_3$ solutions of different concentrations, and the corresponding absorbance (y = 0.01868x- 0.01193) is shown in Fig. S14.

Detection of NO_2^-:

5 mL reacted electrolyte and 0.2 mL NO_2^-chromogenic agent were mixed together, and then the mixed solution stood for 10 min. The absorbance of the mixed solution was detected at 540 nm. The standard curve was obtained by linear fitting of $NaNO_2$ solutions of different concentrations, and the corresponding absorbance (y = 0.46967x- 0.00467) is shown in Fig. S15.

(The preparation of NO_2^-chromogenic agent is as follows: 2.0 g p-aminobenzenesulfonamide was added in 25 mL water, and then 5 mL phosphoric acid and 0.1 g N-(1-naphthyl)-ethylenediamine dihydrochloride were added. Finally, the obtained solution was diluted to 50 mL.

^{15}N isotope labeling experiment：The PEC-NITRR experiment was carried out with $^{15}NaNO_3$ and $^{14}NaNO_3$ as the reactants, respectively. Before the reaction, Ar gas was passed through the electrolytic cell for 1 h to eliminate the interference of air. The concentrated electrolyte was finally measured by ^{1}H NMR.

1.7. Computational methods

The yield (aq) was calculated by the following formula:

$$V_{NH_3} = (C_{NH_3} \times V) / (A \times t)$$

$$V_{NO_2^-} = (C_{NO_2^-} \times V) / (A \times t)$$

NO_3^- conversion rate (aq) was calculated by the following formula：

$$NO_3^- \text{ conversion} = \Delta C_{NO_3^-} / C_0 \times 100\%$$

The NH_3 selectivity (aq) was calculated by the formula:

$$NH_3 \text{ selectivity } (S_{NH_3}) = C_{NH_3} / \Delta C_{NO_3^-} \times 100\%$$

The NO_2^- selectivity (aq) is calculated by the formula:

$$NO_2^- \text{ selectivity } (S_{NO_2^-}) = C_{NO_2^-} / \Delta C_{NO_3^-} \times 100\%$$

C_{NH_3} and $C_{NO_2^-}$ are the concentrations of NH_3 and NO_2^-, respectively, C_0 is the initial concentration of NO_3^-, and $\Delta C_{NO_3^-}$ is the concentration difference before and after the reaction. V, A and t are electrolyte volume, catalyst area and reaction time, respectively.

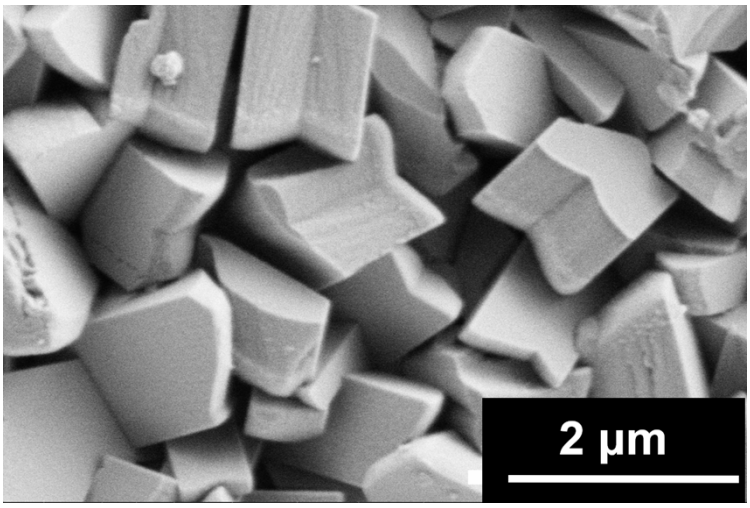

Fig. S1 SEM image of p-$BiVO_4$.

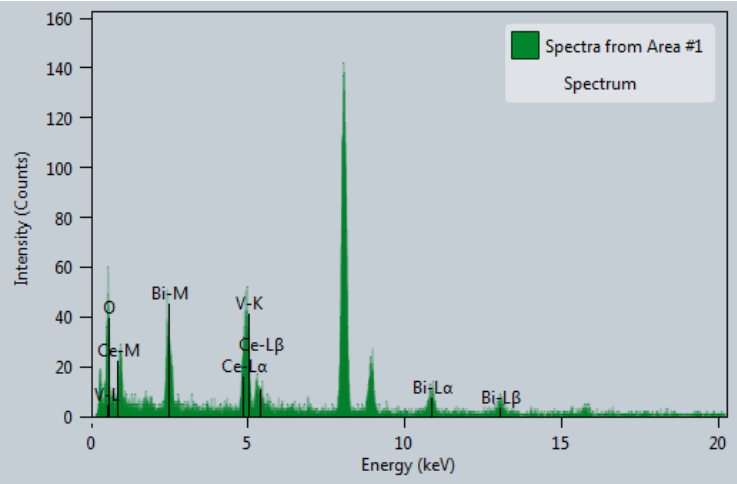

Fig. S2 The EDS spectra of Ce-$BiVO_4$.

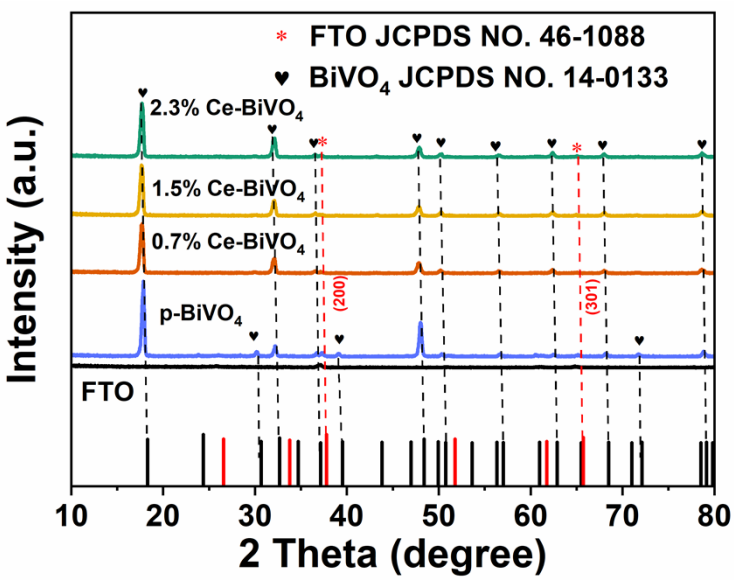

Fig. S3 XRD patterns of p-$BiVO_4$ and xCe-$BiVO_4$.

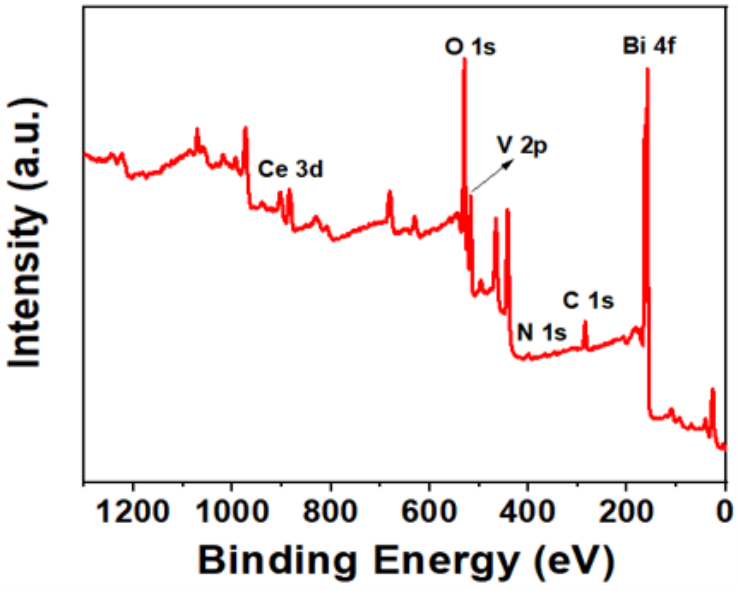

Fig. S4 XPS full scan spectrum of Ce-$BiVO_4$.

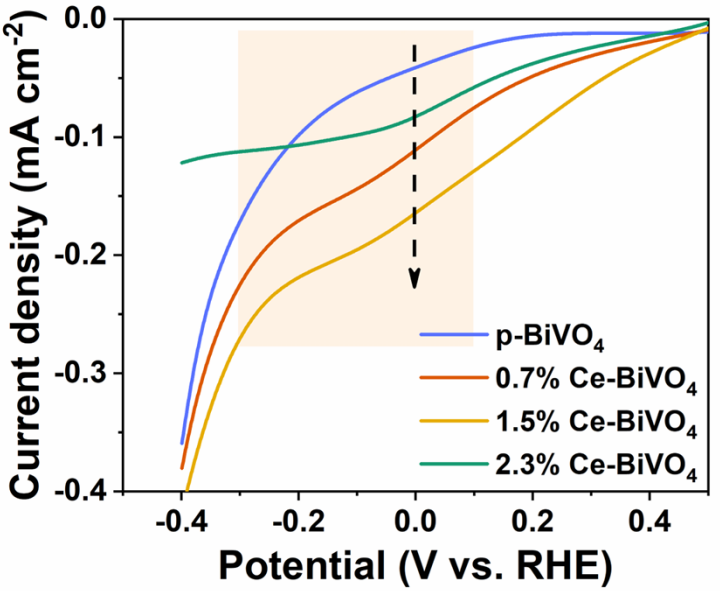

Fig. S5 LSV curves of p-$BiVO_4$ and xCe-$BiVO_4$ in 0.5 M Na_2SO_4 containing 0.15 M NO_3^- under dark condition.

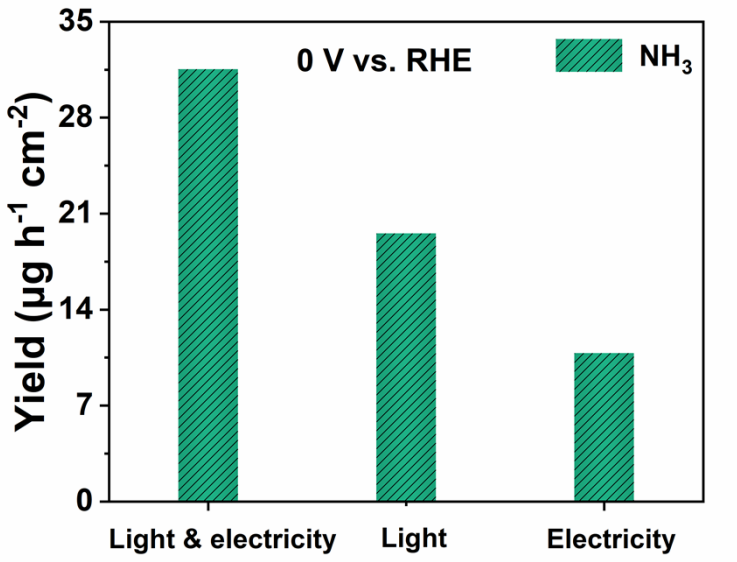

Fig. S6 NH_3 yields of 1.5% Ce-$BiVO_4$ under the different reaction conditions.

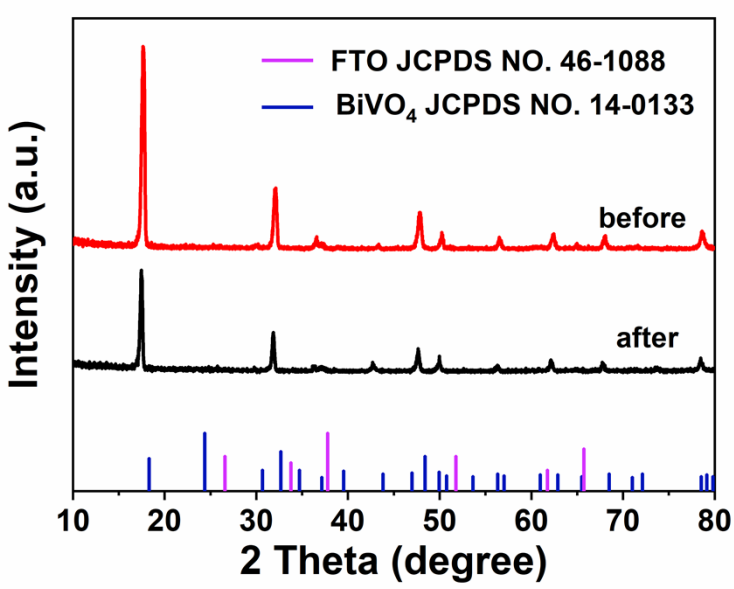

Fig. S7 XRD patterns of 1.5% Ce-$BiVO_4$ before and after reaction.

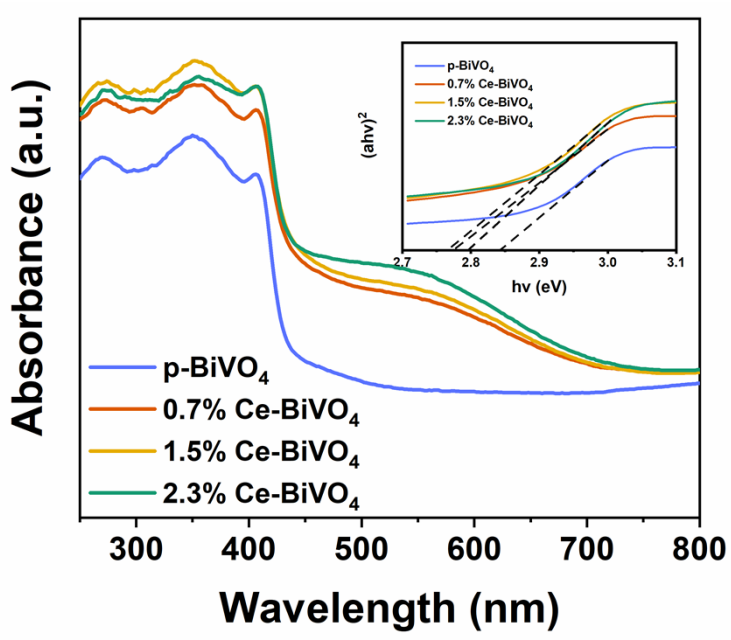

Fig. S8 UV-vis absorption spectra and Tauc plots of p-$BiVO_4$ and xCe-$BiVO_4$.

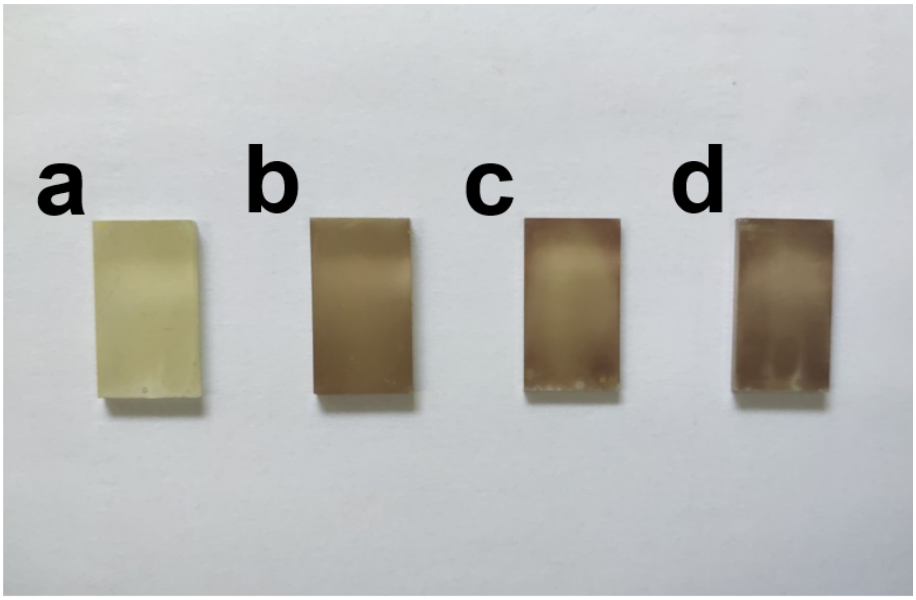

Fig. S9 Digital photos of (a) p-$BiVO_4$, (b) 0.7% Ce-$BiVO_4$, (c) 1.5% Ce-$BiVO_4$, (b) 2.3% Ce-$BiVO_4$.

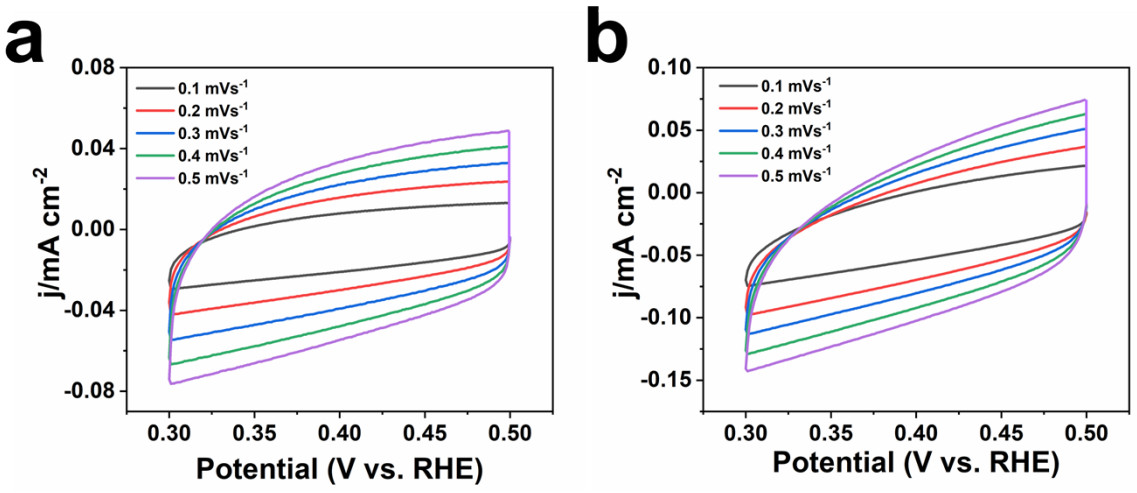

Fig. S10 Electrochemical double layer capacitance (C_{dl}) measurements of (a) p-$BiVO_4$ and (b) 1.5% Ce-$BiVO_4$ at scan rates of 0.1, 0.2, 0.3, 0.4 and 0.5 mVs^{-1}.

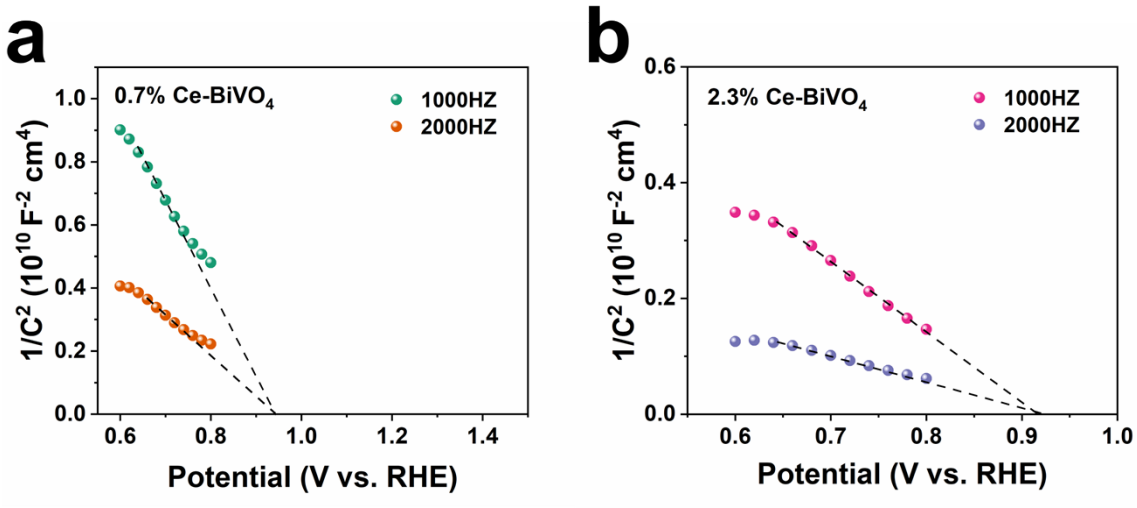

Fig. S11 Mott-Schottky plots at 1000 Hz and 2000 Hz: (a) 0.7% Ce-$BiVO_4$, (b) 2.3 % Ce-$BiVO_4$.

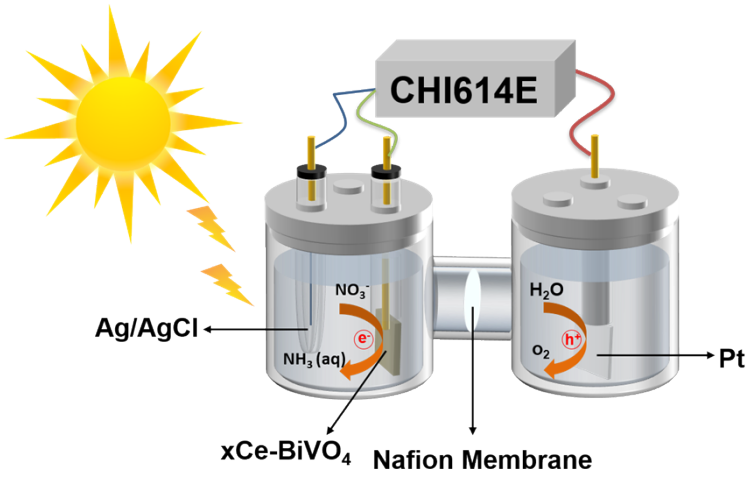

Fig. S12 Schematic illustration of the H-type electrolytic cell for the PEC-NIRR reaction.

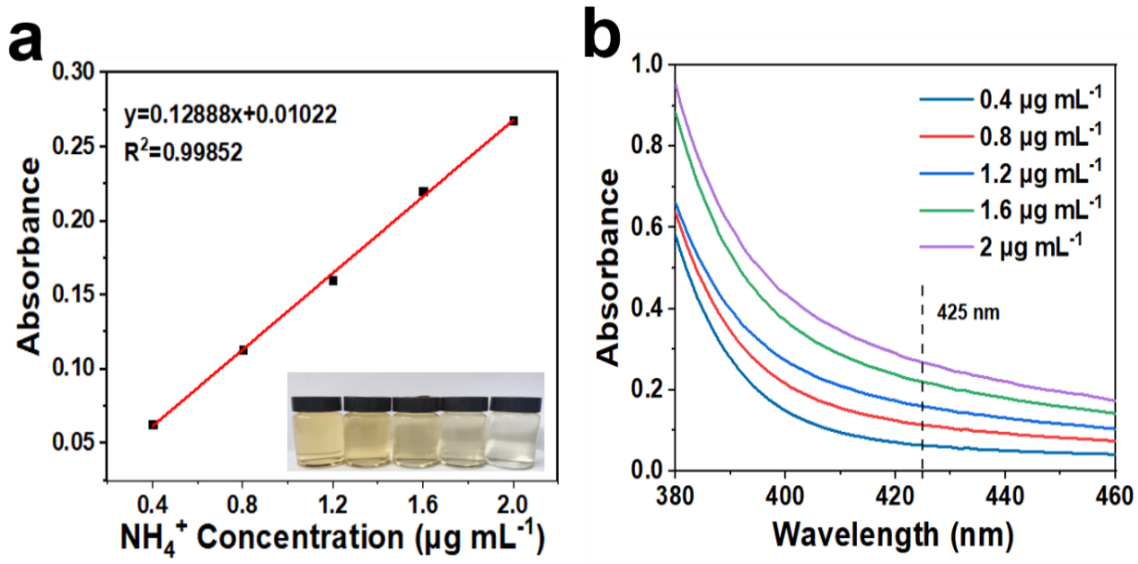

Fig. S13 (a) Standard absorbance curves of different NH_3 concentration and their color reaction after adding Nessler's reagent, (b) the corresponding absorbance curve.

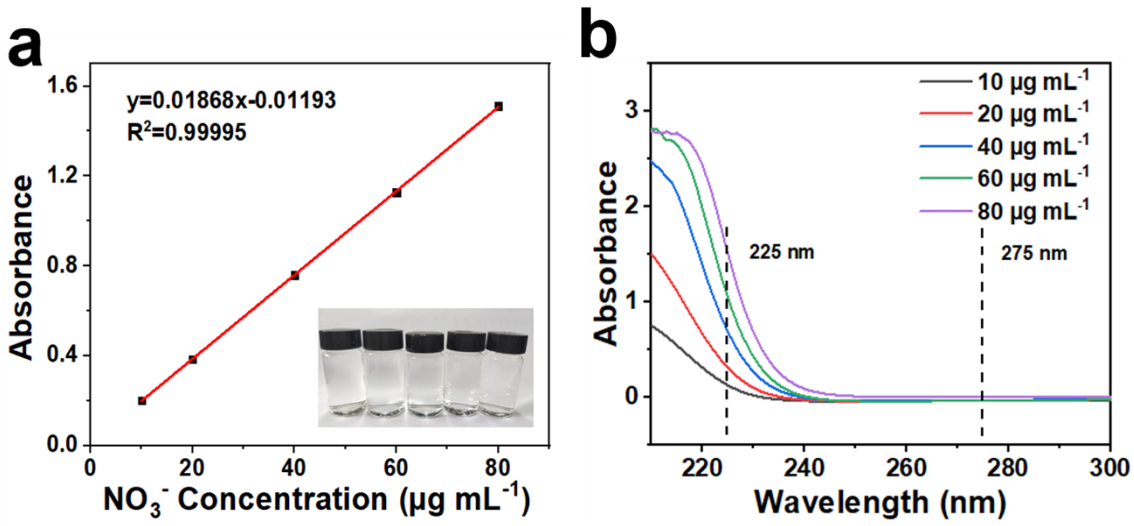

Fig. S14 Standard absorbance curves of different NO_3^- concentration, (b) the corresponding absorbance curve.

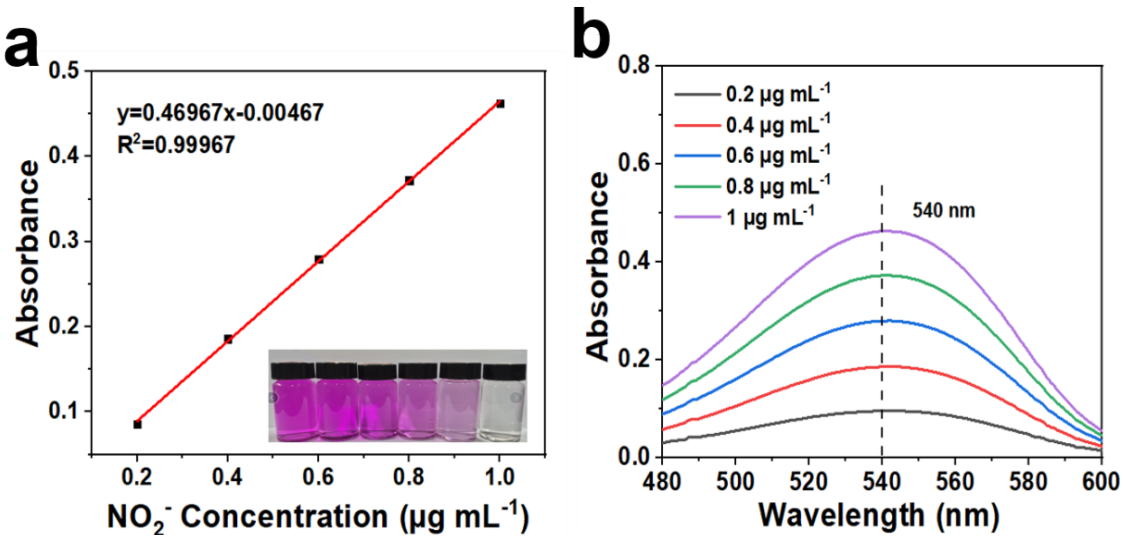

Fig. S15 (a) Standard absorbance curves at different NO_2^- concentration and the corresponding color reaction, (b) the corresponding absorbance curve.

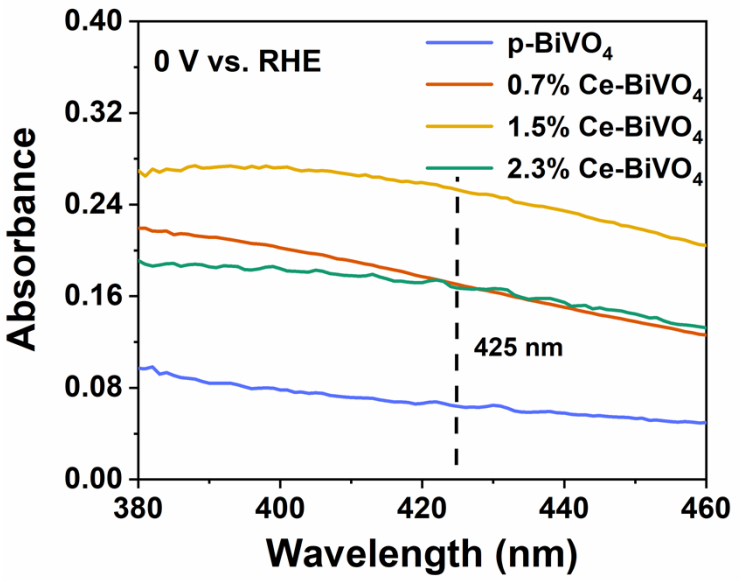

Fig. S16 UV-Vis absorption curves and the corresponding absorbance values at 425 nm of the reacted electrolyte for xCe-$BiVO_4$.

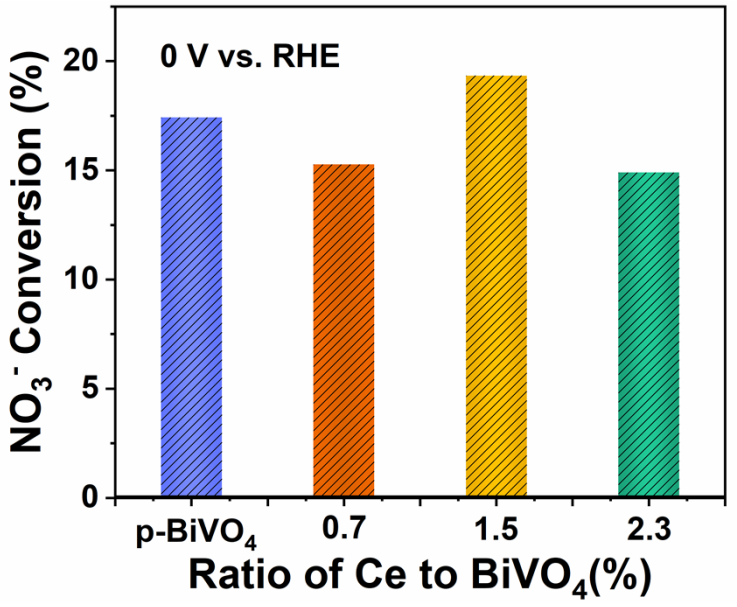

Fig. S17 NO_3^- conversion rate of xCe-$BiVO_4$.

Table S1 For various electrocatalysis (EC) and photocatalysis (PEC) catalysts summary of representative experiments on NH_3 yield without the externally applied potentials (0 V vs. RHE).

Optimal condition	Catalyst	Process	NH_3 Yield	Ref.
0 V vs. RHE	VP/VF	EC	8.35×10^{-11} mol·s^{-1}·cm^{-2}	S1
	Pd	EC	24.3 μg mg$^{-1}_{cat}$ h^{-1} (4.86 μg h^{-1} cm^{-2})	S2
	OVs-PdCu-2	EC	55.54 μg h^{-1} mg$_{cat}^{-1}$ (4.44 μg h^{-1} cm^{-2})	S3
	V-TiO_2/CC	EC	3.4 μg h^{-1} cm^{-2}	S4
	1.5% Ce-$BiVO_4$	**PEC**	**31.54 μg h^{-1} cm^{-2}**	**This work**

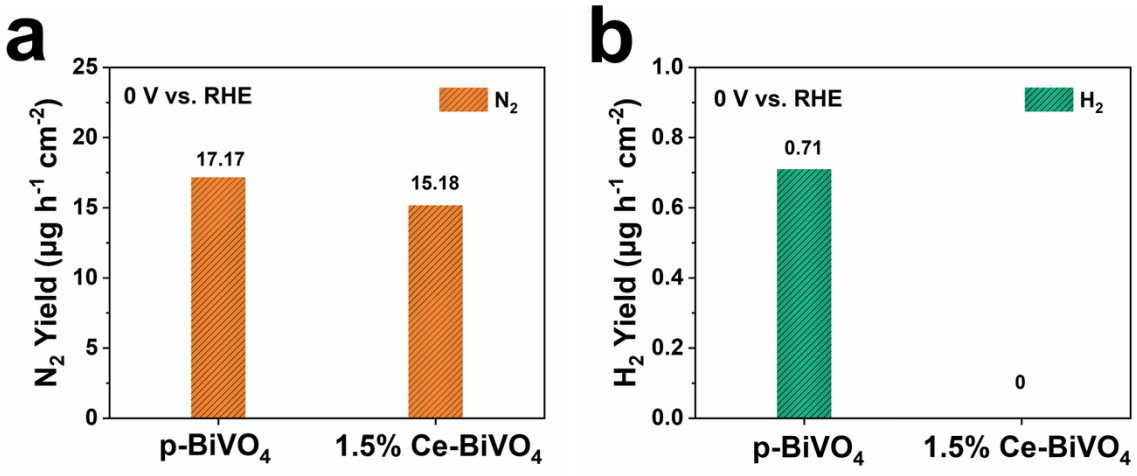

Fig. S18 Yield of samples (p-$BiVO_4$ and 1.5% Ce-$BiVO_4$) (a) N_2, (b) H_2.

References

1 P. Wei, Q. Geng, A.I. Channa, X. Tong, Y. Luo, S. Lu, G. Chen, S. Gao, Z. Wang and X. Sun, Electrocatalytic N_2 reduction to NH_3 with high Faradaic efficiency enabled by vanadium phosphide nanoparticle on V foil, *Nano Res*., 2020, **13**, 2967-2972.

2 H. Zhao, D. Zhang, H. Li, W. Qi, X. Wu, Y. Han, W. Cai, Z. Wang, J. Lai and L. Wang, Exposure of definite palladium facets boosts electrocatalytic nitrogen fixation at low overpotential, *Adv. Energy Mater*., 2020, **10**, 2002131.

3 Z. Wang, X. Wu, J. Liu, D. Zhang, H. Zhao, X. Zhang, Y. Qin, N. Nie, D. Wang and J. Lai, Ordered Vacancies on the Body-Centered Cubic PdCu Nanocatalysts, *Nano Lett.* 2021, **21**, 9580-9586.

4 X. Ma, Q. Zhang, L. Gao, Y. Zhang and C. Hu, Atomic-Layer-Deposited Oxygen-Deficient TiO_2 on Carbon Cloth: An Efficient Electrocatalyst for Nitrogen Fixation, *ChemCatChem*, 2022, **14**, e202200756.